Solvation suppression of ion recombination in gas discharge afterglow

R. Kh. Amirov,[1,2,*] A. V. Lankin,[1,2,†] and G. E. Norman[1,2,3,‡]

[1]*Joint Institute for High Temperatures, Russian Academy of Sciences, 13 Izhorskaya Street, Moscow 125412, Russia*
[2]*Moscow Institute of Physics and Technology, 9 Institutskiy Pereulok, Dolgoprudny, Moscow Region 141701, Russia*
[3]*National Research University Higher School of Economics, 20 Myasnitskaya Ulitsa, Moscow 101000, Russia*

(Received 10 July 2017; published 12 March 2018)

An effect which suppresses recombination in ion plasmas is considered both theoretically and experimentally. Experimental results are presented for the ion recombination rate in fluorine plasma, which are obtained from data for the gas discharge afterglow. To interpret them, a suppression factor is considered: ion solvation in weakly ionized plasma. It is shown that the recombination process has a two-stage character with the formation of intermediate metastable ion pairs. The pairs consist of negative and positive ion-molecular clusters. A theoretical explanation is given for the slowing down of the ion recombination with the increase of the Coulomb coupling compared to the ion recombination rate calculated in the ideal plasma approximation. The approximate similarity of the recombination rate of the ion temperature and concentration and reasons for the slight deviation from the similarity are elucidated.

DOI: 10.1103/PhysRevE.97.033202

I. INTRODUCTION

Ion plasmas are formed in dense electronegative media at pulse discharges for a nanoseconds' time as a result of the electrons' attachment to atoms and molecules. The lifetime of the plasma formed is about tens of microseconds or more. Ion recombination processes are essential for systems of direct nuclear energy conversion [1–3], at initiation of chain and nonchain chemical lasers [4–6], at the breakdown of development in electronegative gases [7,8], at the dielectric strength restoration of transformer oil after electrical breakdown in high-voltage equipment [9], at discharges in air [10–12], etc. Ion recombination processes should be taken into account in the description of plasma composition, hydrodynamics, and chemical reactions kinetics, in particular, in the case of fast, strongly nonequilibrium phenomena.

It is well known that the three-body recombination of ions is valid for moderate gas pressures and low concentrations of ions. The recombination constant k is satisfactorily described by the Nathanson model [13], which is a development of the Thomson model. However, as both the concentration of ions and gas pressure increase, deviation from the Thomson model can appear.

It has been pointed out [14,15] that there is no clear understanding how the increased concentration of ions affects the recombination rate. The question of recombination of ions of high concentration in molecular gases, where cluster ions can be formed [16], also remains open. Stakhanov [17] conjectured substantial slowing of ion recombination in a cluster plasma.

Experimental methods for investigating three-body ion-ion recombination are effective in the case of a low degree of ionization [15] and ion concentrations of less than 10^8 cm^{-3}. At the same time, ion-ion recombination determines plasma decay with a high concentration of strongly electrically negative gases such as F_2, in which, due to the high rate of electron attachment to molecules [15], an ion plasma is formed in the early afterglow. The recombination of fluorine ions is one of the channels for the formation of atomic fluorine. The rate of formation of atomic fluorine is an important factor that determines the efficiency of pulsed chemical HF and DF-CO_2 chain reaction lasers.

Recombination processes in ion plasmas have some peculiarities which differ from the recombination in electron-ion plasmas. The condition is sufficient for the recombination of two ions when the distance between them becomes small enough to make possible a tunneling transfer of an electron from the negative to the positive ion [18], whereas the presence of a third particle or an environment to capture the excess energy is necessary for the recombination of an electron and an ion. The ion number density in ion plasmas is usually several orders of magnitude less than the neutrals' number density. Therefore, the number of ion-neutral collisions is much greater than the number of collisions between ions [18]. In particular, this fact, together with the relatively low temperature of ions and neutrals, creates favorable conditions for complex cluster ion production [16]. Ion solvation can become a factor which lowers the recombination rate value with respect to that in ideal plasmas.

The molecular dynamics (MD) method [19–21] can be applied to study both ion plasma and cluster ions in it. The MD method is widely used to calculate properties of diverse ion and molecular systems: electrolytes, ion systems, cluster ions, and solvate complexes.

The process of electron-ion relaxation is treated by the MD method for plasmas of sulfur and fluorine ions [22]. It is shown that the classical Spitzer formula describes this process satisfactorily if screening only by electrons (not by ions) is

*amirovravil@yandex.ru
†Alex198508@yandex.ru
‡genri.norman@gmail.com

taken into account in the calculation of the Coulomb integral. The same problem is considered as a more general statement and for a wider parameter set in Ref. [23].

The formation of $(CsI)_nCs^+$ clusters is treated in Ref. [24]. The results of both direct experimental investigation of their structures and density functional theory (DFT) -based modeling results are presented, which turn out to be in good agreement with each other. The formation and properties of clusters composed of water molecules and argon atoms are studied theoretically in Ref. [25], where the classical MD method is used. A remarkable difference is shown between the attachment cross sections of the two species to the clusters formed. Argon clusters are found to be close to spherical symmetry even for a small number of atoms included, whereas a remarkable deviation is observed for water clusters. The same method is used in Ref. [26] to study the formation and properties of solvate I_3^- ion-based clusters. The violation of the symmetry of these solvate clusters is considered in liquid media and the gas phase.

Molecular dynamics modeling is used to describe the formation of ion solvate shells in solutions of complex ruthenium compounds; a significant difference is shown for space distribution functions which appear in solutions with different types of haloid anions [27]. I_2^- ion solvation is considered in the carbon dioxide medium; the influence of the solvate shell formation on the ion optical properties is studied in Ref. [28]. The solvation of an astatine ion in an aqueous solution is studied in Ref. [29]; an interparticle potential is used which is derived from nonempirical quantum calculations. Classical trajectory calculations are applied; a threshold law for ion-neutral-neutral three-body recombination processes has been derived and numerically confirmed in Ref. [30]. Structure and properties of ion-molecular clusters are considered in Ref. [31,32] which are formed in the gaseous phase of water vapors; thermodynamic parameters are calculated for the ions $H_3O^+(H_2O)_n$ and $OH^-(H_2O)_n$ for a number of n. Formation and structure of solvate complex of hydroperoxide anion in the aqueous medium is studied in Ref. [33].

Despite the numerous works on the MD modeling of properties of charged particles in various media, the problem of cluster ion formation and its influence on the processes in the gaseous phase is not studied sufficiently. We consider the problem in this paper for the example of ion recombination in the molecular fluorine medium.

Solvation suppression of the ion recombination is considered in this paper. Experimental data for the recombination process in fluorine plasma of the gas discharge afterglow are presented in Sec. II. They point to the fact that lowering of the recombination rate value with respect to that in ideal plasmas takes place even in the weakly nonideal plasmas. Sections III–V are devoted to the analysis of the influence of ion solvation and ion-neutral cluster formation on the recombination in ion plasmas. The MD method is used in Sec. III. It is shown that the most stable ion-molecule clusters $F^-(F_2)_{12}$ and $F_2{}^+(F_2)_{12}$ with icosahedral close packing are formed quickly because the F_2 number density exceeds the ion number density by several orders of magnitude. The characteristic time τ_r of the spontaneous unimolecular decay of the isolated cluster pair $F^-(F_2)_{12}F_2{}^+(F_2)_{12}$ in the recombination products is calculated in Sec. IV. The time τ_i of the inverse disintegration of the cluster pair into cluster ions $F^-(F_2)_{12}$ and $F_2{}^+(F_2)_{12}$ due to collisions with the environment particles is considered in Sec. V. An analytical model is suggested in Sec. VI, which explains experimental results for the fluorine plasmas.

II. EXPERIMENTAL DATA PROCESSING

The recombination constants of ion plasma are determined by the time dependence of ion concentration in a decaying plasma from the measurements of conductivity. In the experiment, the conductivity of afterglow plasma produced by a high-power nanosecond-pulsed discharge in F_2 at $P = 60$–250 torr is measured. A 16.5-cm-long sapphire tube with an inner diameter of 18 mm is used as a discharge device. The voltage amplitude of a high-voltage nanosecond discharge detected by a capacitive divider on the high-voltage electrode is 125 kV, while the current amplitude, measured with the use of a shunt resistor placed close to the discharge tube, ranges from 2.8 to 1.0 kA, depending on pressure. The discharge duration is about 35 ns, with a leading edge of 2 ns and a trailing edge of 10–15 ns. Synchronized measurements of voltage and current allow one to determine the energy input in the discharge gap and the characteristic electron density in the discharge and to estimate the plasma temperature in the late afterglow [34].

Electron concentration in the discharge can be evaluated by the formula

$$n_e = J/eV_{\rm dr}(E/P)S_0, \tag{1}$$

where $V_{\rm dr}$ is the electron drift velocity, S_0 is the discharge tube cross-section area, and e is the electron charge. For a nanosecond discharge current of $J \approx 1.0$–2.8 kA and a characteristic reduced electric field voltage of $E/P \approx 30$–130 V/(cm torr), using the known values of the electron drift velocity in F_2, the calculated electron concentration [34] is $5 \times (10^{14}$–$10^{15})$ cm^{-3}. Similar values are estimated from the energy input data [34]. When the discharge is turned off, the electrons are cooled in inelastic collisions within nanoseconds or even faster and are effectively involved in attachment reactions. Upon reaching energies of 1.5–2 eV, electrons efficiently enter into reactions of dissociative attachment $e + F_2 \rightarrow F^- + F$ with a characteristic value of the rate constant [15] of 10^{-9} m^3 s^{-1}. At the gas densities considered, the characteristic time of attachment is a few nanoseconds.

Methods of determining ion plasma conductivity, formed after the end of a nanosecond discharge, consist in the following: Low current probe pulses are applied to the discharge gap; the duration of these pulses is such that the voltage drop U_1 in electrode sheath regions due to the formation of volume charge is much less than the voltage U on the discharge gap, which is the parameter to be measured. In this case, the intensity of the electric field produced in plasma does not not lead to the negative ions' destruction.

If we assume that $U_1 < 0.1U$, then the condition for a probe pulse length is determined by the expression $t < 1.4 \times 10^{-7}(L/ju_i)^{1/2}$ s, where L is the discharge gap length in cm, u_i is the ion mobility in cm^2/(V s), and j is the current density in a probe pulse [34] in A/cm^2. According to estimates, the duration of a probe pulse should not exceed 1 μs for the range of parameters considered. For a current flow with a density $j < 10$ mA/cm^2, which is the case in this experiment, and ion

TABLE I. Rate constants for ion-ion recombination in fluorine ion plasmas.

n_i (cm^{-3})	Γ	k (cm^3/s)
Pressure 60 torr, $T = 300$ K		
4.06×10^{12}	0.143	7.2×10^{-8}
8.24×10^{12}	0.181	6.9×10^{-8}
1.63×10^{13}	0.227	6.4×10^{-8}
4.14×10^{13}	0.310	5.5×10^{-8}
Pressure 100 torr, $T = 500$ K		
1.32×10^{13}	0.127	2.60×10^{-8}
2.63×10^{13}	0.160	2.48×10^{-8}
5.30×10^{13}	0.202	2.33×10^{-8}
1.04×10^{14}	0.253	2.13×10^{-8}
1.29×10^{14}	0.272	2.05×10^{-8}

concentration of $n_i \geqslant 10^{13}$ cm^{-3}, the reduced field strength E/N_a in a plasma column satisfies the inequality $E/N_a \leqslant j/en_i K N_a \approx 10^{-16}$ V cm^2, where N_a is the concentration of neutral molecules. For these values of E/N_a, the electron concentration is less than the ion concentration by at least five orders of magnitude and the contribution of electrons to the conductivity can be neglected, taking into account their mobility [35].

The conductivity is measured for the afterglow time of $\tau = 2 \times (10^{-6}$–$10^{-5})$ s. Since a late afterglow is investigated, when most of the ions have recombined, the assumption of the value of the plasma temperature determined from the total energy input is correct at the plasma decay stages considered [34]. The effect of a high ion concentration on conductivity is calculated by taking into account ion-ion collisions together with collisions with gas molecules and relaxation correction, which takes into account strong coupling of the ion plasma [36]. When determining the ion concentration, the characteristic composition of ions is taken into account. To obtain ion recombination constants, we use the experimental data [34,37,38]. The results are presented in Table I, where the Coulomb coupling parameter $\Gamma = (4\pi n_i/3)^{1/3}(e^2/kT)$. When determining recombination, the temperature of the recombining plasma is assumed to be different from room temperature and is determined by the heat capacity of the gas and the specific energy input to the nanosecond discharge, which is strongly dependent on gas pressure [34].

III. ION COMPOSITION

The F_2 plasma conductivity decay is defined only by the processes with fluorine ions [34] at the pressures and afterglow times considered. That is why it is used in Sec. II to find the recombination rate values. The main positive ion is F_2^+, its number density exceeding that of F^+ considerably [39,40]. The ion F^- is the main negative ion [39–41].

Ion solvation is calculated in two steps. The interaction potentials of fluorine ions with the fluorine molecule are found first. Quantum calculations are performed for F^-F_2 and $F_2^+F_2$ systems in the DFT approximation with the CPMD package [42]. The basis contains 389 220 plane waves with $E = \hbar^2k^2/2m$ up to 90 Ry. Valence electrons are treated in the Kohn-Sham equations explicitly, two core electrons being included in the pseudopotential for each atom. The exchange-correlation functional is taken in the Perdew-Burke-Ernzerhof generalized gradient form. The computations are carried out for the isolated cubic box, the edge l being from 1 to 20 Å. The interactions are averaged over all directions and the resulting pair potentials $U(r)$ are presented in the spherically symmetric form approximated by the sum of the Lennard-Jones potential and polarization long-range r^{-4} attraction

$$U(r) = 4\epsilon[(\sigma/r)^{12} - (\sigma/r)^6] - \alpha/r^4, \qquad (2)$$

where $\epsilon = 1.46$ eV, $\sigma = 2.48$ Å, and $\alpha = 10.29$ eV Å^4 for F^- and $\epsilon = 1.9$ eV, $\sigma = 2.5$ Å, and $\alpha = 10.29$ eV Å^4 for F_2^+. Test computations of the fluorine atom and negative ion are performed with the same problem definition as for F^-F_2 and $F_2^+F_2$. The energy of both atomic fluorine and its negative ion becomes constant and independent of the box size for $l > 8$ Å. The value of the energy for F^- turns out to be lower by 4.7 eV than for the F atom. It is even larger than the reference value of 3.4 eV for the atomic fluorine affinity.

TABLE II. Energies of clusters formed by ions F^- and F_2^+.

n	$F^-(F_2)_n$	$F_2^+(F_2)_n$
1	1.65	2.07
2	3.30	4.15
3	4.97	6.24
4	6.64	8.34
5	8.33	10.45
6	10.02	12.56
7	11.64	14.63
8	13.00	16.52
9	14.54	18.54
10	15.43	20.05
11	15.65	21.00
12	16.70	22.56

In the second step, the potentials (2) are used to study the equilibrium structure and stability of the clusters $F_2^+(F_2)_n$ and $F^-(F_2)_n$ at different temperatures. The method of classical MD is applied. The Lennard-Jones potential $U_{LJ}(r) = 4\epsilon_{F2}[(\sigma_{F2}/r)^{12} - (\sigma_{F2}/r)^6]$, with $\epsilon_{F2} = 0.0097$ eV and $\sigma_{F2} = 3.35$ Å, is used for the interaction between fluorine molecules.

To start simulations, a particle configuration is created with a random distribution of molecules within a certain radius around the ion. A gradient descent method is applied to obtain a configuration which is used as an initial one for a short MD run to heat the cluster and equilibrate it at 500 K. The temperature is close to the experimental one. Then the cluster is cooled to zero temperature. The binding energy obtained is taken as the cluster energy. The cluster energy values calculated are given in Table II.

Modeling results show that the successive addition of F_2 to both $F_2^+(F_2)_n$ and $F^-(F_2)_n$ up to $n = 11$ is an exothermal process with an energy release of about 1 eV. The energy exceeds the thermal energy of the gas molecules considerably. Therefore, the clusters formed are stable and further augmentation of F_2 continues. The only exception is $F^-(F_2)_{11}$, where ten molecules form the inner layer, but the eleventh one is

displaced to the external layer. The augmentation energy of the eleventh molecule is only 0.28 eV. However, the augmentation energy of the twelfth molecule is 1.06 eV and the cluster returns to the one-layer ball and forms an icosahedral close-packed structure. The augmentation energies for $F_2{}^+$ clusters are slightly larger than for F^- up to $n = 12$. The augmentation energies for $n > 12$ are close to the thermal energy and the two-layer clusters formed are not stable.

Since the cross section of the clusters is about 26 $Å^2$, the molecule attachment time does not exceed 5 ns in the experimental conditions considered. It is much smaller than the ion recombination time; therefore, the ions are mostly $F^-(F_2)_{12}$ and $F_2{}^+(F_2)_{12}$ in fluorine plasma.

IV. SPONTANEOUS UNIMOLECULAR DECAY OF THE ISOLATED CLUSTER PAIR

The binding energy of the cluster pair $F^-(F_2)_{12}F_2{}^+(F_2)_{12}$ is $E_0 = 1.3$ eV, calculated in the same way as for cluster ion energies. Despite the positive value of the binding energy, the cluster pair $F^-(F_2)_{12}F_2{}^+(F_2)_{12}$ is metastable with respect to the unimolecular decay. The ions F^- and $F_2{}^+$ are able to get thermally over the potential barrier between them in the cluster pair and recombine, forming three fast fluorine atoms

$$F^-(F_2)_{12}F_2{}^+(F_2)_{12} \rightarrow 24F_2 + 3F.$$

The process is stochastic in nature and can be calculated by the classical MD method. The average lifetime of the isolated cluster pair is found for MD runs with respect to the spontaneous decay. The procedure can be subdivided into three steps.

The first one is modeling of a cluster pair. Two cluster ions of opposite sign are created as described in the preceding section. Then they are spaced at a certain distance. A configuration is found by the gradient descent method, which corresponds to the local minimum of the potential energy. The configuration obtained is used as an initial one for the MD simulation of the cluster ion pair, which is the second step.

The MD run starts from heating and equilibration of the cluster ion pair at a specified temperature. It is a short trajectory. The main part is an equilibrium trajectory until the moment of the recombination. The event is supposed to happen when ions F^- and $F_2{}^+$ approach each other at a critical distance r_{cr} equal to the average distance between an ion and a molecule of the solvate shell in a cluster ion. The event defines the lifetime of the cluster ion pair for that particular initial state. The lifetime values do not depend on r_{cr} in the interval $r_{cr}/\sigma \simeq 10^{-1}$–1.

The third step is necessary since the decay process has a stochastic character as the dynamic memory time [21] at the numerical integration is much less than the lifetime studied. Therefore, a number of equilibrium MD runs is implemented for each temperature to learn the kinetics of the decay into recombination products. The initial equilibrium sets of particle coordinates and velocities correspond to one and the same temperature but differ from each other microscopically. Therefore, the lifetime obtained for each MD run is a unique one. Only the average lifetime τ_r has a physical meaning. The results obtained are presented in Fig. 1. The size of the open circles corresponds to the error bars of the results. The temperature

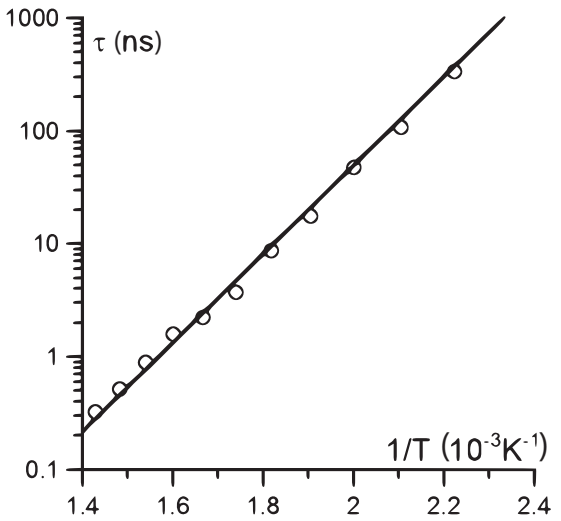

FIG. 1. Dependence of the lifetime of the isolated metastable ion pair $F^-(F_2)_{12}F_2{}^+(F_2)_{12}$ on the inverse temperature. Open circles are the results of MD simulations and the solid line is Eq. (3).

dependence is described in Arrhenius form

$$\tau_r^{-1} = k_r = B\exp(-E_r/k_BT), \tag{3}$$

where $B = 1.4 \times 10^{15}$ s^{-1}, the activation energy $E_r = 0.8$ eV, and k_r is in s^{-1}.

It follows from Fig. 1 that the straight line fit is valid up to a temperature of about 700 K. Computations for higher temperatures were not performed because of a technical modeling problem: Clusters disintegrated during the time period needed to prepare and equilibrate clusters to study unimolecular decay.

V. REVERSE DISINTEGRATION OF THE METASTABLE CLUSTER PAIR INTO FREE CLUSTER IONS

A. Collisional disintegration

An isolated cluster pair was considered in the preceding section. However, collisions of a cluster pair with the ion plasmas' environment can result in the inverse disintegration of the cluster pair into two cluster ions before the spontaneous recombination of $F_2{}^+$ and F^- ions inside the cluster pair takes place. To calculate the characteristic time τ_i of the cluster pair's disintegration into free cluster ions, one can equate the kinetic equilibrium constant with the thermodynamic one for the reaction

$$F^-(F_2)_{12}F_2{}^+(F_2)_{12} \leftrightarrow F^-(F_2)_{12} + F_2{}^+(F_2)_{12}.$$

In the kinetic approach, the numbers of cluster pairs which are disintegrated and generated per unit time are equated to each other

$$k_i n_p = k' n^+ n^-, \tag{4}$$

where n_p and $n^+ = n^-$ are number densities of cluster pairs and ions, $k_i = \tau_i^{-1}$ is a reverse disintegration constant, and k' is a rate constant of the formation of metastable cluster ion pairs from free cluster ions. The constant can be calculated from the Nathanson model for ion recombination at Γ values not largely exceeding 0.1.

In the thermodynamic approach, the relation between number densities of cluster pairs and ions is given for the weakly coupled plasma by the equation

$$K = (\gamma_+\gamma_-/\gamma_p)(n_+n_-/n_p), \tag{5}$$

where K is a thermodynamic equilibrium constant and γ_+, γ_-, and γ_p are fugacity coefficients for positive and negative ions and ion pairs, respectively. Since experiments [34,37] deal with relatively low gas densities at small Γ, the fugacity coefficient for cluster pairs $\gamma_p = 1$ and fugacity coefficients for cluster ions can be estimated in the Debye approximation

$$\gamma_\pm(\Gamma) = \gamma_+(\Gamma) = \gamma_-(\Gamma) = \exp(-\sqrt{6}\Gamma^{3/2}/2). \tag{6}$$

It was pointed out in Ref. [34] that the recombination rate decrease correlates with the increase of fugacity coefficients γ in weakly coupled ion plasmas.

The determination of τ_i is reduced to the calculation of the thermodynamic equilibrium constant K. In this case, we can determine the value of n_+n/n_p from Eq. (5), substitute it in Eq. (4), and relate τ_i to the recombination constant k'.

B. Equilibrium constant

The constant K can be presented in the ideal gas approximation as

$$K = (2\pi kT\mu/h^2)^{3/2} Z_+^{\text{in}} Z_-^{\text{in}}/Z_p, \tag{7}$$

where μ is the reduced mass of the positive and negative cluster ions in the pair, Z_+^{in} and Z_-^{in} are internal vibrational-rotational partition functions of positive and negative ions, respectively, and Z_p is an internal partition function of the metastable ion cluster pair which can be defined as $Z_p = Z_p^C Z_p^+ Z_p^-$, where Z_p^C is a partition function of vibrations of two ion clusters which the pair is composed of and Z_p^+ and Z_p^- are internal vibrational-rotational partition functions of positive and negative cluster ions in the pair. If one neglects the difference between $Z_+^{\text{in}}, Z_-^{\text{in}}$ and Z_p^+, Z_p^- and sets $Z_+^{\text{in}} = Z_p^+$ and $Z_-^{\text{in}} = Z_p^-$, Eq. (7) is reduced to

$$K = (2\pi kT\mu/h^2)^{3/2} 1/Z_p^C. \tag{8}$$

Calculation of Z_p^C is performed in the quasiclassical approximation for the model interaction of two cluster ions

$$U_{ii}(r) = \begin{cases} -e^2/4\pi\varepsilon_0 r, & r > e^2/E_0 \\ \infty, & r < e^2/E_0, \end{cases} \tag{9}$$

where ε_0 is the dielectric constant and $E_0 = 1.4$ eV as found in Sec. III. In this case Z_p^C is calculated as

$$Z_p^C = (32\sqrt{2}\varepsilon_0^3 h^3)^{-1} e^6 \mu^{3/2} \int_{-E_0}^{-\Delta E} [|\varepsilon|^{-5/2} - |E_0|^{-5/2}] \exp(-\varepsilon/kT) d\varepsilon, \tag{10}$$

where ΔE is a parameter which restricts the contribution of the pair states with low binding energies. The result depends on ΔE rather weakly. The estimate $\Delta E \approx 4.6 \times 10^{-7} (n_-)^{1/3}$ (where ΔE is in eV and n_- is in cm^{-3}) is used by analogy with electron-ion plasmas [43]; other restrictions are given in Refs. [44,45]. Using Eqs. (8) and (10), one finally obtains

$$K = 128\varepsilon_0^3 e^{-6} (\pi kT E_0)^{3/2} F^{-1}(\Gamma, T, E_0), \tag{11}$$

where

$$F(\Gamma, T, E_0) = \int_{-1}^{-2\Gamma kT/E_0} [|x|^{-5/2} - 1] \exp(-E_0 x/kT) dx. \tag{12}$$

The equilibrium constant obtained numerically can be approximately presented in the temperature range from 300 to 700 K as

$$K = K_0 \exp(-E_1/kT), \tag{13}$$

where $E_1 = 1.4$ eV.

C. Reverse disintegration time

The relation (4) between rate constants of reverse disintegration of pairs and recombination is in ideal plasmas

$$k_i = k'K \tag{14}$$

and in nonideal plasmas

$$k_i = \tau_i^{-1} = k'K\gamma_p/\gamma_+\gamma_-. \tag{15}$$

VI. RECOMBINATION RATE

The metastable cluster pair can either inversely disintegrate into free cluster ions or recombine according to the unimolecular decay. The effective recombination mechanism passes through the reversible formation of the intermediate metastable pairs of cluster ions

$$F^-(F_2)_{12} + F_2{}^+(F_2)_{12} \leftrightarrow F^-(F_2)_{12}F_2{}^+(F_2)_{12} \rightarrow 24F_2 + 3F.$$

The effective recombination rate is described by the equation

$$k = k'/[1 + \tau_r/\tau_i], \tag{16}$$

where k' is the metastable pair's formation rate and τ_r and τ_i are characteristic times of the unimolecular decay and inverse disintegration into free ions, respectively. Taking into account Eqs. (3), (11), (15), (16), and (13), one obtains

$$\begin{aligned} k \equiv k(\Gamma, T) &= k'\{1 + k'K\tau_r(T)\gamma_\pm^{-2}\}^{-1} \\ &= k'\{1 + (k'K_0/B)\exp[(E_r - E_1)/k_BT] \\ &\quad \times \exp(\sqrt{6}\Gamma^{3/2})\}^{-1}. \end{aligned} \tag{17}$$

The appearance of the $(E_r - E_1)/k_BT$ factor breaks the similarity of k with respect to Γ. However, the proximity of the E_r value to E_1 can reduce the difference between values of k for different temperatures at one and the same value of Γ. Nevertheless, this difference can be resolved experimentally. Equation (17) is valid in the temperature range from 300 to about 700 K. It follows from the procedures of evaluation of E_1 and E_r values.

A comparison of the recombination rate constant (17) with the experimental data obtained is presented in Fig. 2 for the discharge afterglow ion plasma in fluorine. Molecular dynamics values for the cluster parameters are used. The theoretical model agrees with measurements of both absolute values and the Γ dependence. The results for temperatures of 300 and 500 K and pressures of 60 and 100 torr turn out to be close to each other. Despite this closeness, the calculations reproduce a slight difference between sets of the experimental

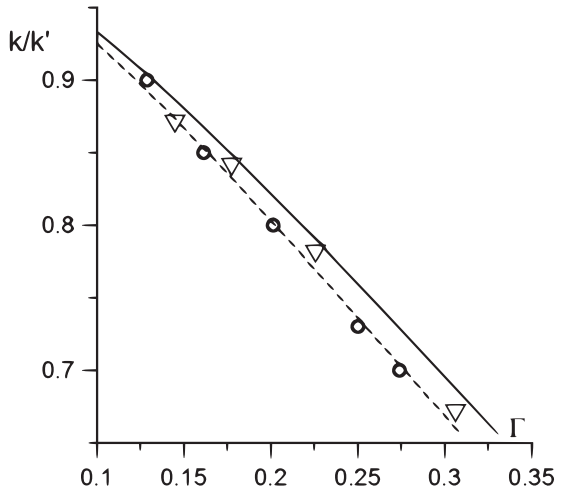

FIG. 2. Ratio of the ion recombination rate for the discharge afterglow plasma in fluorine to the ion recombination rate in the limit of the ideal plasmas. The data from Table I are shown by ◯ for $P = 100$ torr and $T = 500$ K and ▽ for $P = 60$ torr and $T = 300$ K. The model (17) is represented by a solid line for $T = 300$ K and $P = 60$ torr and by a dotted line for $T = 500$ K and $P = 100$ torr.

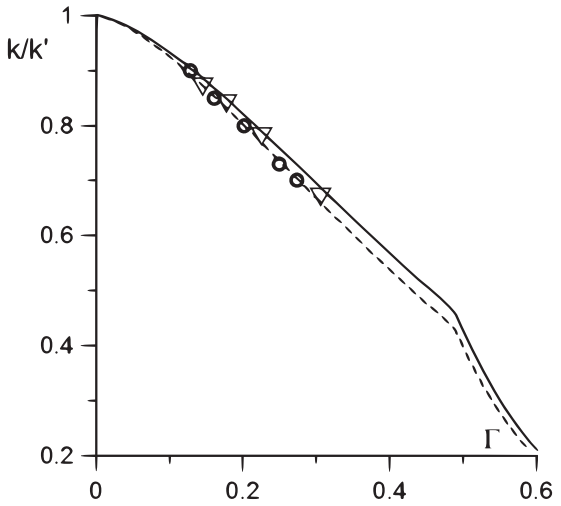

FIG. 3. Ratio of the ion recombination rate for the discharge afterglow plasma in fluorine to the ion recombination rate in the limit of the ideal plasmas. The data from Table I are shown by ◯ for $P = 100$ torr and $T = 500$ K and ▽ for $P = 60$ torr and $T = 300$ K. The model (17) is represented by a solid line for $T = 300$ K and $P = 60$ torr and by a dotted line for $T = 500$ K and $P = 100$ torr. See the text for the break.

points for conditions of 100 torr and 500 K and of 60 torr and 300 K. The agreement of the difference points to the reliability of the quantum mechanical calculations performed for the binding energies.

The model developed uses the Debye approximation essentially for the ion fugacity coefficient estimation. It limits the model applicability by the value $\Gamma \sim 0.5$ since the Debye approximation predicts pressure up to these coupling values [46].

Effects appear at larger values of Γ which are connected with both a change of the ion fugacity coefficient dependence on Γ and the deviation of k' in Eq. (17) from the Nathanson model. The important effect is a formation of the area of multiparticle fluctuation near the ionization limit [43,47] which should be taken into account in the k' calculation. Its influence results in the additional Γ dependence of the rate constant k: A break appears at $\Gamma = 0.5$ (Fig. 3) if the effect is taken into account in the same form as for the electron-ion plasma [47–49]. The deviation from Eq. (17) grows with the increase of Γ.

VII. CONCLUSION

Experimental data for the ion-ion recombination rate and their theoretical explanation were presented in weakly coupled fluorine ion plasmas of the gas discharge afterglow. Both the measurements and the theory point to the suppression of recombination in ion plasmas with respect to the conventional ideal plasma formulas. The suppression increases with the increase of the Coulomb coupling parameter Γ. The following issues were highlighted theoretically.

(i) Ion recombination for the discharge afterglow plasma in fluorine is slowed down by the solvation of ions and passes through the reversible formation of the intermediate metastable pairs of cluster ions.

(ii) The Γ dependence of the recombination rate at small values of Γ is caused by the dependence of the equilibrium number density of metastable ion pairs on the ion fugacity, which is defined only by Γ in the Debye approximation.

(iii) The approximate similarity of the recombination rate of the ion temperature and number density was elucidated. The slight deviation from the similarity was also defined. It points to the reliability of the quantum mechanical calculations performed for the binding energies.

(iv) A formula was suggested which takes ion solvation into account and describes suppression of the ion recombination rate.

ACKNOWLEDGMENTS

The article was prepared within the framework of the Basic Research Program at the National Research University Higher School of Economics and supported within the framework of a subsidy by the Russian Academic Excellence Project "5-100" (G.E.N.). The research was made possible by the Government of the Russian Federation, Grant Agreement No. 05.Y09.21.0018 (A.V.L.).

[1] M. Prelas, *Nuclear Pumped Lasers* (Springer International, Cham, 2016).

[2] R. D. Yung, W. Well, and G. Miley, Appl. Phys. Lett. **28**, 194 (1976).

[3] M. A. Prelas, M. A. Akerman, F. P. Boody, and G. H. Miley, Appl. Phys. Lett. **31**, 428 (1977).

[4] F. Kannri, H. Inagaki, and M. Obara, Appl. Phys. Lett. **48**, 266 (1986).

[5] V. Apollonov, A. Belevtsev, S. Kazantsev, A. Saifulin, and K. Firsov, Quantum Electron. **31**, 629 (2001).

[6] V. Apollonov, A. Belevtsev, S. Kazantsev, A. Saifulin, and K. Firsov, Quantum Electron. **30**, 207 (2001).

[7] W. Wang, A. B. Murphy, M. Rong, H. M. Looe, and J. W. Spencer, J. Appl. Phys. **114**, 103301 (2013).

[8] P. Robin-Jouan and M. Yousfi, Plasma Sci. Technol. **9**, 690 (2007).

[9] M. S. Apfel'baum, Surf. Engin. Appl. Electrochem. **47**, 35 (2011).

[10] A. Napartovich and N. Aleksandrov, Phys. Usp. **36**, 107 (1993).

[11] N. Aleksandrov, S. Kindysheva, M. Nudnova, and A. Y. Starikovskiy, J. Phys. D **43**, 255201 (2010).

[12] A. V. Shavlov, Phys. Lett. A **373**, 3959 (2009).

[13] B. M. Smirnov, *Theory of Gas Discharge Plasma*, Springer Series on Atomic, Optical, and Plasma Physics Vol. 84 (Springer International, Cham, 2015).

[14] M. Flanerry, J. Phys. B **18**, L531 (1985).

[15] M. Flannery, in *Applied Atomic Colision Physics*, edited by E. W. McDaniel and W. L. Nighan (Academic, New York, 1983), Vol. 3, p. 393.

[16] B. Smirnov, *Complex Ions* (Gordon and Breach, Amsterdam, 1985).

[17] I. Stakhanov, J. Exp. Theor. Phys. Lett. **18**, 114 (1973).

[18] B. Smirnov, *Negative Ions* (McGraw-Hill, London, 1982).

[19] D. Rapaport, *The Art of Molecular Dynamics Simulation*, 2nd ed. (Cambridge University Press, Cambridge, 2004).

[20] M. Tuckerman, *Statistical Mechanics: Theory and Molecular Simulation* (Oxford University Press, Oxford, 2010).

[21] G. Norman and V. Stegailov, Math. Models Comput. Simul. **5**, 305 (2013).

[22] L. X. Benedict, J. N. Glosli, D. F. Richards, F. H. Streitz, S. P. Hau-Riege, R. A. London, F. R. Graziani, M. S. Murillo, and J. F. Benage, Phys. Rev. Lett. **102**, 205004 (2009).

[23] G. Dimonte and J. Daligault, Phys. Rev. Lett. **101**, 135001 (2008).

[24] S. Kruckeberg, D. Schooss, M. Maier-Borst, and J. H. Parks, Phys. Rev. Lett. **85**, 4494 (2000).

[25] J. Lengyel, A. Pysanenko, V. Poterya, P. Slavicek, M. Farnik, J. Kocisek, and J. Fedor, Phys. Rev. Lett. **112**, 113401 (2014).

[26] F. S. Zhang and R. M. Lynden-Bell, Phys. Rev. Lett. **90**, 185505 (2003).

[27] I. Josefsson, K. Eriksson, H. Rensmo, and M. Odelius, J. Struct. Dyn. **3**, 023607 (2016).

[28] B. M. Ladanyi and R. Parson, J. Chem. Phys. **107**, 9326 (1997).

[29] F. Real, A. Severo, P. Gomes, Y. G. Martinez, T. Ayed, N. Galland, M. Masella, and V. Vallet, J. Phys. Chem. Phys. **144**, 124513 (2016).

[30] J. Perez-Rios and C. H. Greene, J. Chem. Phys. **143**, 041105 (2015).

[31] S. Shevkunov, Colloid J. **70**, 630 (2008).

[32] S. Shevkunov, Colloid J. **66**, 506 (2004).

[33] M. E. Tuckerman, D. Anick, and M. Zhonghua, J. Phys. Chem. B **118**, 7937 (2014).

[34] R. Amirov, Habilitation thesis, JIHT RAS, 2000, available at http://www.dissercat.com/content/relaksatsionnye-protsessy-initsiiruemye-nanosekundnymi-razryadami-v-molekulyarnykh-gazakh.

[35] D. Syers, in *Atomic and Molecular Processes*, edited by D. Bates (Academic, New York, 1962), p. 240.

[36] E. M. Lifshitz and L. P. Pitaevskii, *Physical Kinetics* (Butterworth-Heinemann, Oxford, 1981).

[37] R. K. Amirov, E. I. Asinovskii, S. V. Kostyuchenko, and V. V. Markovets, High Temp. **25**, 793 (1987).

[38] R. K. Amirov, E. I. Asinovskii, S. V. Kostyuchenko, and V. V. Markovets, Institute for High Temperatures, Academy of Sciences of the USSR Report No. 8-200, 1986 (unpublished).

[39] H. Chen, R. Center, D. Trainor, and W. Fyfe, J. Appl. Phys. **48**, 2297 (1977).

[40] M. Vasile, J. Appl. Phys. **51**, 2503 (1987).

[41] J. Bardsley and J. Waridehra, J. Chem. Phys. **78**, 7227 (1983).

[42] CPMD, Car-Parrinello molecular dynamics, an *ab initio* electronic structure and molecular dynamics program, available at http://cpmd.org/documentation.

[43] A. Lankin and G. Norman, J. Phys. A: Math. Theor. **42**, 214032 (2009).

[44] M. Capitelli and D. Giordano, Phys. Rev. A **80**, 032113 (2009).

[45] A. Calisti and B. Talin, Contrib. Plasma Phys. **51**, 524 (2011).

[46] R. G. Bystryi, Y. S. Lavrinenko, A. V. Lankin, I. V. Morozov, G. E. Norman, and I. M. Saitov, High Temp. **52**, 475 (2014).

[47] A. Lankin and G. Norman, Contrib. Plasma Phys. **49**, 723 (2009).

[48] A. Lankin, J. Exp. Theor. Phys. **107**, 870 (2008).

[49] A. Lankin and G. Norman, J. Phys. A: Math. Theor. **42**, 214042 (2009).